Journal of The
Electrochemical Society

The Electrochemical Society
Advancing solid state & electrochemical science & technology

PEDOT for Sensitive Electrochemical Detection of Trimetazidine Hydrochloride in Biological Fluids: Synthesis, Characterization and Mechanism Insights

To cite this article: Abdelqader El Guerraf *et al* 2020 *J. Electrochem. Soc.* **167** 167525

View the article online for updates and enhancements.

You may also like

- Four equal-intensity foci generated by a Cantor–Thue–Morse zone plate
Tian Xia, Shubo Cheng and Shaohua Tao
- Amrubicin encapsulated PLGA NPs inhibits the PI3K/AKT signaling pathway by activating PTEN and inducing apoptosis in TMZ-resistant Glioma
Muhammad Younis, Sana Shaikh, Khawar Ali Shahzad et al.
- Drug delivery by SiC nanotubes as nanocarriers for anti-cancer drugs: investigation of drug encapsulation and system stability using molecular dynamics simulation
Atousa Faizi, Zahra Kalantar and Seyed Majid Hashemianzadeh

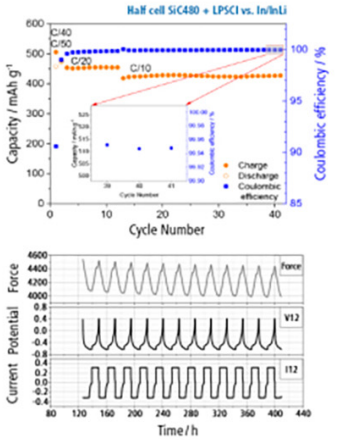
The New PAT-Cell-Solid!

EL-CELL®
electrochemical test equipment

Cycle Solid-State Batteries Under Controlled Pressure of up to 300 MPa (6 mm Diameter)!



- Adjust and measure a force of up to 9000 N on the cell stack!
  Force adjustment possible throughout the entire experiment
- Built-in force, and temperature sensors!
  With optional gas pressure sensor and gas in- and outlet
- PAT-Solid-Core for easy assembly and reproducible results!
  Press and cycle solid-state batteries with 6 or 10 mm electrode diameter
- Cableless and highly sealed battery test cell!
  For precise long-term measurements of solid-state cell chemistries



Learn more on our product website: Scan me!

Download the data sheet (PDF): Scan me!

Or contact us directly:
+49 40 79012-734
sales@el-cell.com
www.el-cell.com

This content was downloaded from IP address 161.9.196.133 on 23/09/2026 at 08:08

Journal of The Electrochemical Society, 2021 **167** 167525
1945-7111/2021/167(16)/167525/11/$40.00 © 2021 The Electrochemical Society ("ECS"). Published on behalf of ECS by IOP Publishing Limited
All rights, including for text and data mining, AI training, and similar technologies, are reserved.

PEDOT for Sensitive Electrochemical Detection of Trimetazidine Hydrochloride in Biological Fluids: Synthesis, Characterization and Mechanism Insights

Abdelqader El Guerraf,[1] Nurgul K. Bakirhan,[2,z] Sana Ben Jadi,[3] Mohammed Bazzaoui,[3] Yalcin Ozkan,[4] El Arbi Bazzaoui,[1] and Sibel A. Ozkan[5,z]

[1]*Laboratory of Applied Chemistry and Environment, Faculty of Sciences, Mohammed First University, 60000 Oujda, Morocco*
[2]*University of Health Sciences, Gülhane Faculty of Pharmacy, Department of Analytical Chemistry, 06018 Ankara, Turkey*
[3]*Materials and Environmental Laboratory, Faculty of Sciences, Ibn Zohr University, 80000 Agadir, Morocco*
[4]*University of Health Sciences, Gulhane Faculty of Pharmacy, Department of Pharmaceutical Technology, 06018 Ankara, Turkey*
[5]*Ankara University, Faculty of Pharmacy, Department of Analytical Chemistry, 06100 Ankara, Turkey*

Trimetazidine hydrochloride (TMZ), well-known by its unique and interesting pharmacological properties, has been investigated by several electrochemical techniques using Poly(3,4-ethylenedioxythiophene) coated glassy carbon electrode (GCE). The preparation of the modified electrode was achieved by the electrodeposition of PEDOT in two different media and the obtained film has been characterized by scanning electron microscopy (SEM) and infrared spectroscopy (FTIR). The electrochemical analysis of TMZ was then studied by cyclic, differential pulse and square wave voltammetric methods in solutions of different pH values and results have shown that square wave voltammetry (SWV) is the most suitable one for the analytical characterization. The oxidation of TMZ was irreversible and was a process under diffusion control. Besides, Model compounds and molecules were also used in this study to describe the possible oxidation mechanism of TMZ. In this contribution, the main objective is the possible practical use of the proposed method, thus, the electrochemical detection of TMZ by SWV was carried out in biological samples, such as human serum and urine. Under the optimum condition in phosphate buffer at pH 3.0, linear calibration curves were obtained for all studied media (supporting electrolyte, urine and serum). Important parameters, namely, precision, accuracy, limit of detection (LOD) and limit of quantification (LOQ) were reported, and good sensitivity, reproducibility and repeatability were obtained. Furthermore, recovery values of almost 100% were found for pharmaceuticals and biological samples, suggesting that the sensor can be used in practical applications.
© 2021 The Electrochemical Society ("ECS"). Published on behalf of ECS by IOP Publishing Limited. [DOI: 10.1149/1945-7111/abd5fa] All rights, including for text and data mining, AI training, and similar technologies, are reserved.

Manuscript submitted October 10, 2020; revised manuscript received December 1, 2020. Published January 4, 2021.

Supplementary material for this article is available online

Trimetazidine (TMZ) dihydrochloride [1-(2,3,4-trimethoxybenzyl)-piperazine dihydrochloride] (Scheme 1) is a highly effective, well-tolerated drug, usually known for its antianginal effect,[1] correcting the disorder of ion pumps and sodium/potassium cross membrane flow, maintains cellular homeostasis,[2] used in ischemia of neurosensorial tissues as in Meniere's disease,[3] and acts as a scavenger of oxygen radicals.[4] TMZ is a dibasic compound used in several countries as a safe cellular anti-ischemic agent without any hemodynamic effects.[1] It reaches the maximum concentration in the serum after about 5 h from oral administration while the steady state concentration is reached after about 60 h. Trimetazidine is eliminated mainly in the urine in an unchanged form and the average half-life is 7 h. Until these days, the mechanism of action of TMZ remains hard to explain, however, its role as an antioxidant and its ability to preserve high energy phosphate metabolism has been already reported.[4,5]

Although numerous analytical methods have been previously used for the determination and quantification of TMZ in biological fluids and pharmaceutical formulations, including UV–visible spectrophotometry,[6] flow injection chemiluminescence,[7] GC/MS,[8] LC/MS,[9] HPLC method with fluorescence[10] and electrochemical[11] detectors and reversed-phase (RP)HPLC,[12] these techniques require complex sample preparations, high-cost instrumentation and they are unwieldy and time-consuming.

Since their discovery in the seventies, conducting polymers (CPs) have attracted enormous interest due to their huge field of applications. These novel materials are usually used in catalysis, electromagnetic shielding, organic solar cells, secondary batteries and as protective coatings of oxidizable metals against corrosion.[13–17] Among various organic CPs, polythiophene (PT) and its derivatives were considered to be the most interesting and frequently investigated because of their high electrical conductivity, good chemical stability, non-toxicity and ease of synthesis.[18–20] These properties have allowed the development of many applications of poly(3,4-ethylenedioxythiophene) (PEDOT), including sensors.[21,22]

Unlike the usual conducting polymers such as polypyrrole and polyaniline which could be obtained in aqueous media, PT derivatives are generally prepared by electrochemical oxidation of the corresponding monomer in an organic medium.[23–25] Several reports dedicated to the preparation of PEDOT films in different organic solvents were published, we note especially, those related to acetonitrile or propylene carbonate where electroactive, stable and adherent coatings were obtained on the surface of an inert electrode (generally platinum).[25–28]

On the other hand, the poor solubility of PT and derivatives in conventional aqueous media,[29,30] resulting especially from the rigidity of the polymeric backbone and the strong inter-chain interaction, has been a great impediment to their electropolymerization, and thus represents a serious drawback for several industrial applications.

The need to use such polymers in industrial applications has led to much research devoted to solve this problem. In this context, homogeneous and very adherent PT film has been successfully elaborated on platinum electrode in aqueous perchloric acid.[31] Furthermore, several authors have reported the possible synthesis of PEDOT films in aqueous micellar mediums,[32–34] this latter can provide a great environment for the solubilization of the EDOT monomer. In the mid-90, Sakmeche et al.[35] have succeeded the elaboration of PEDOT on platinum electrodes from an aqueous micellar medium of sodium dodecyl sulfate (SDS). The obtained film has shown a well-organized structure and the oxidation potential of the monomer decreased enormously compared to the one observed when using acetonitrile solution, this has resulted from the presence of

[z]E-mail: nurgulk44@gmail.com; ozkan@pharmacy.ankara.edu.tr

surfactant micelles, which create hydrophobic and hydrophilic regions at the metal/solution interface, thus, inducing an electrocatalytic effect.

In the following study, we report our detailed investigation related to the electrooxidation analyses of TMZ using different electrochemical methods, namely, cyclic, differential pulse and square wave voltammetric techniques, since they offer a rapid analysis, simple operation and low-cost instrumentation. PEDOT films were obtained, after a preliminary study, on glassy carbon electrodes by electrochemical synthesis from organic and aqueous micellar solutions. Analytical characterization of the sensor was undertaken for the direct determination of TMZ in urine and serum samples.

Experimental

Chemicals.—3,4-Ethylenedioxythiophene ($C_6H_6O_2S$, 97%), tetrabutylammonium hexafluorophosphate ($C_{16}H_{36}F_6NP$, 98%) ($TBAPF_6$), sulfuric acid (H_2SO_4, 99%), phosphoric acid (H_3PO_4, 85%), acetic acid ($C_2H_4O_2$, 99%), sodium phosphate monobasic dihydrate (NaH_2PO_4, $2H_2O$), sodium phosphate dibasic (Na_2HPO_4), sodium acetate ($C_2H_3NaO_2$), sodium dodecyl sulphate ($NaC_{12}H_{25}SO_4$), acetonitrile (C_2H_3N, 99.9%) and methanol (CH_3OH, 99.9%) were obtained from Sigma-Aldrich and used as received. Trimetazidine hydrochloride ($C_{14}H_{24}Cl_2N_2O_3$) was purchased from Farma-Tek, mirtazapine ($C_{17}H_{19}N_3$) from Nobel and anisole (C_7H_8O) was obtained from Sigma.

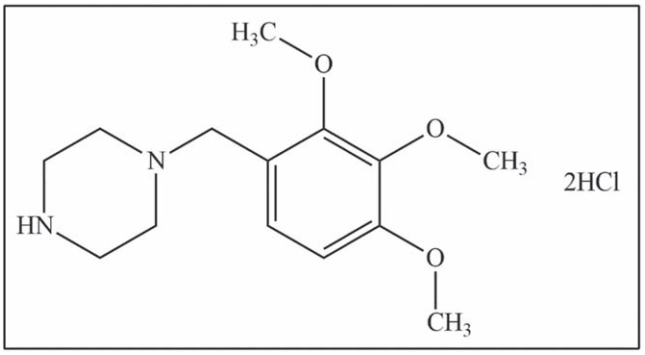
Buffer and TMZ stock solutions, namely, sulfuric acid (pH 1.3) phosphate buffer (pH 2.2; 3.0; 5.8; 6.8 and 7.7), acetate buffer (pH 4.2 and 5.1) and TMZ (1×10^{-3} M) solutions were prepared with highly purified water from PURELAB purification system and stored in the refrigerator (4 °C) to prevent their degradation.

H_3PO_4, NaH_2PO_4–$2H_2O$ and Na_2HPO_4 were used with different amounts for the preparation of phosphate buffers while acetic acid and sodium acetate were used in the case of acetate buffers. The related pH values were fixed with sodium hydroxide (Sigma) using pH meter Model 538 (WTW, Austria) with a combined glass electrode–reference electrode in an accuracy of pH ± 0.05.

Electrochemical apparatus.—Voltammetric methods i.e., cyclic voltammetry (CV), square wave voltammetry (SWV) and differential pulse voltammetry (DPV) were performed at room temperature in one-compartment with the three conventual electrodes system using an Autolab potentiostat/galvanostat model PGSTAT101 with pilot integration controlled by NOVA 2.1 software (Fig. 1). The working electrode (WE) was either glassy carbon or boron-doped-diamond (diameter: 3 mm). The auxiliary electrode (AE) was a platinum with spiral-like geometry and all potentials given in this study were referred to Ag/AgCl immersed in saturated KCl solution (3 M).

DPV experiments were conducted under the instrumental conditions of: modulation amplitude 0.025 V; step potential 0.005 V; interval time 0.5 s; modulation time 0.05 s. Moreover, SWV parameters were optimized for a better response, the optimum conditions were: 0.025 V modulation amplitude, 0.01 V step potential and 10 Hz frequency. All experiments were carried at room temperature.

The precision and the accuracy of the developed methods were checked by calculating relative standard deviations (RSD%) at within day (five repetitive experiments) and between days (five repetitive experiments) and was also described in a quantitative fashion by the use of Bias% (relative error). In addition, all experiments were accomplished at least in triplicate with an experimental error not exceed 2% (error bars are presented in calibration curves).



Scheme 1. Structure of trimetazidine.

Preparation of sensor-active materials.—Firstly, glassy carbon and boron-doped-diamond electrodes surfaces were polished mechanically with alumina powder (0.05 μm) over a smooth polishing cloth, cleaned ultrasonically with bi-distilled water and ethanol and then dried at room temperature before use.

PEDOT films were prepared by electropolymerizing of EDOT monomers in two different media using cyclic voltammetry. The first one was acetonitrile (ACN) medium in the presence of {0.1 M $TBAPF_6$ + 0.05 M EDOT} while the second is an aqueous solution containing {0.07 M SDS + 0.05 M EDOT}, this concentration ratio of (EDOT-SDS) has proven to be particularly favorable especially in terms of EDOT solubility.[30]

PEDOT coating was then slowly washed with the synthesis solvent (acetonitrile or bi-distilled water) to remove any attached monomers on the surface and dried at room temperature. The modified electrode was finally placed in the electrochemical cell containing the TMZ solution, followed by the electrochemical investigation.

The cleaning of the modified electrode was carried out periodically after each electroanalytical experiment to remove any adsorbed compound using cyclic voltammetry between −0.25 and 1.8 V (number of scans = 5) in pure supporting electrolyte.

Characterization techniques.—Fourier transform infrared (FTIR) spectrum of PEDOT film was recorded with JASCO 4700 spectrometer in the ranges between 400–2000 cm^{-1}.

Scanning electron microscopy (SEM) images were obtained on a ZEISS EVO 40 instrument. The microscope chamber was maintained at a pressure between 4 and 10 Pa. The distance between the sample and the objective lens remains at 12 mm (working distance) and the SEM filament was operated at variable currents and a voltage of 20 kV using 1000× magnifications. All samples were dried in the oven before experiments.

Interference study, preparation of biological samples and recovery measurements.—The interference of some electroactive compounds was investigated under optimum conditions. Firstly, SW voltammogram of 4×10^{-5} M TMZ was recorded, then, each interferent was added to the cell (containing 4×10^{-5} M TMZ) with different concentrations (4×10^{-5} and 4×10^{-4} M). Concentration ratios (C_{Int}:C_{TMZ}) were 1:1 and 10:1 and SW voltammograms were recorded for each compound. Results were discussed based on the change in the peak currents when adding the interferent compared to the solution of TMZ alone using the relative error (RE%).

Stock solutions of 1×10^{-3} M TMZ in urine and serum samples were prepared after collecting these latter from healthy individuals. The procedure was as follows: 5.4 ml of acetonitrile was mixed with 3.6 ml of urine (or serum) and 1.0 ml of 1×10^{-2} M TMZ in pure water. Acetonitrile, in this case, played a major role as a precipitating agent for removing of protein residues in urine and serum.

Prepared solutions were centrifuged for 10 min at 4500 rpm and clear solutions were then collected carefully. Square wave voltammetry was performed for the analysis of TMZ in these pharmaceutical formulations using PEDOT films in phosphate buffer at pH 3.0. Quantification was realized by means of calibration curves method from the related calibration equations.

Recovery experiments were carried out using the standard addition method, which consists of adding a known amount of TMZ into our biological samples. Averages recovery values were

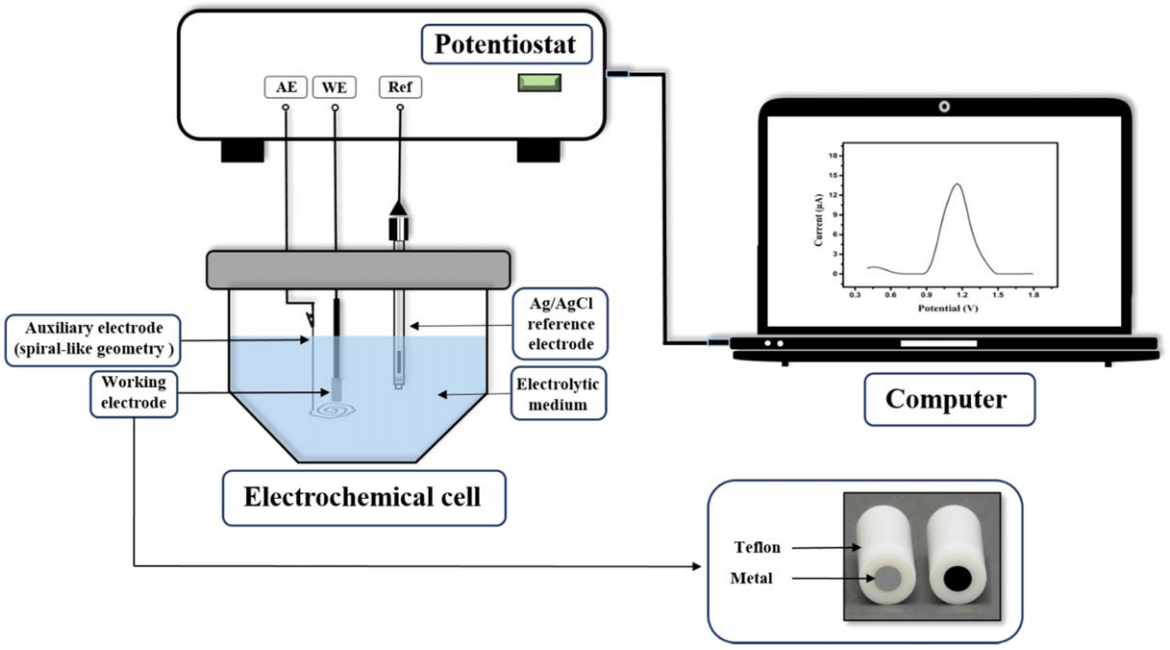


Figure 1. Schematic illustration of the set-up used for the electroanalytical experiments, comprising a single compartment electrochemical cell equipped with a three-electrode system connected to a computer-controlled potentiostat.

calculated after five repetitive experiments using the corresponding regression equation of the previously plotted calibration graph.

Results and Discussion

Preliminary study.—To enhance the understanding of TMZ electrooxidation and in order to get the best analytical results, two electrodes, namely, glassy carbon (GCE) and boron-doped-diamond (BDD) were chosen for the electrochemical detection of the drug. Electrodes were used directly after polishing and cleaning and without any modification.

For the following study, experiments were carried out in various buffer solutions of different pH values using SWV. The selection of this electrochemical method in our analytical studies will be discussed elsewhere.

pH–current relations of TMZ electrooxidation obtained from SWV technique for both electrodes are presented in supplementary Fig. S1 (available online at stacks.iop.org/JES/167/167525/mmedia). The GCE (supplementary Fig. S1A) produced higher current values (up to 12 μA) compared to BDD electrode (supplementary Fig. S1B), where the current does not exceed 4 μA. Consequently, the glassy carbon would make our study more interesting when modified, hence, it will be used in what follows. In addition, phosphate buffer with pH 3.0 has been chosen as the best medium for the electrochemical characterization of TMZ, and that by analyzing the number of peaks, their heights and how well defined are presented. We note that SW voltammograms related to the pH effect will be presented in the following sections to further confirm the choice of this pH value.

In a similar vein, Ghoneim et al.[5] have studied the electrochemical behavior of TMZ on a bare glassy carbon electrode using cyclic and square-wave voltammetry. The characterization was achieved in 0.05 M acetate buffer (pH 5.0) in a potential range of 0–1 V. The voltammograms obtained by the authors contain only a large anodic peak at +0.770 V, which they have assigned to the oxidation dimerization of the –NH center of piperazine ring in the drug molecules through a single two-electron irreversible step. In our case, the voltammetric scan was achieved between −0.25 and 1.8 V, hence, several peaks were observed in the voltammograms. We should note that the structure of TMZ contains numerous active sites that could be oxidized which will give more than one peak. A detailed analytical characterization will be discussed in what follows.

Electrodes modification.—After carefully polishing and cleaning the GCE surface, PEDOT films were electrochemically synthesized using the CV method. The preparation of the polymeric coating was achieved in two different media (organic and micellar) as previously described.

Figure 2 shows the voltamperometric curves of EDOT electropolymerization on GCE, obtained by performing cyclic potential scanning between −0.5 and 1.5 V and between −0.5 and 1.2 V vs Ag/AgCl for organic and aqueous micellar solution respectively and with a scan rate of 100 mV s^{-1}.

In the case of ACN solution containing {0.1 M $TBAPF_6$ + 0.05 M EDOT} and during the first potential scan, an anodic wave at 1.2 V was observed at the working electrode (Fig. 2A) correspond to the oxidation of the monomer and the formation of the first layer of the PEDOT/ACN polymer. During successive potential sweepings, two anodic and cathodic peaks appeared at about 0.56 V and 0.22 V and assigned to the oxidation and the reduction of the deposit respectively.

On the other hand, the electrosynthesis in aqueous micellar medium (Fig. 2B) produced a similar voltammogram to the one observed in the first case, with a shift of potential to more negative values. We observed during the first voltammetric scan, a rapid increase in the anodic current around 0.78 V, which corresponds to the EDOT oxidation and the beginning of PEDOT/SDS formation. We should note an important decrease in the oxidation potential of the EDOT monomer when using SDS medium, this is generally attached to the presence of the anionic surfactant in the solution which generates a different interaction of this anion with the monomer compared to the organic medium containing $TBAPF_6$.[30]

Furthermore, by comparing the obtained current values in the two media, we clearly notice that the voltammogram recorded in organic solution has higher values (>1.7 mA) than the one of micellar solution (≈0.7 mA) which make the polymer prepared in the first medium a better coating in terms of conductivity. In a similar vein, the intensity of the anodic peak associated with the oxidation of the polymer for both voltammograms increases as the number of cycles

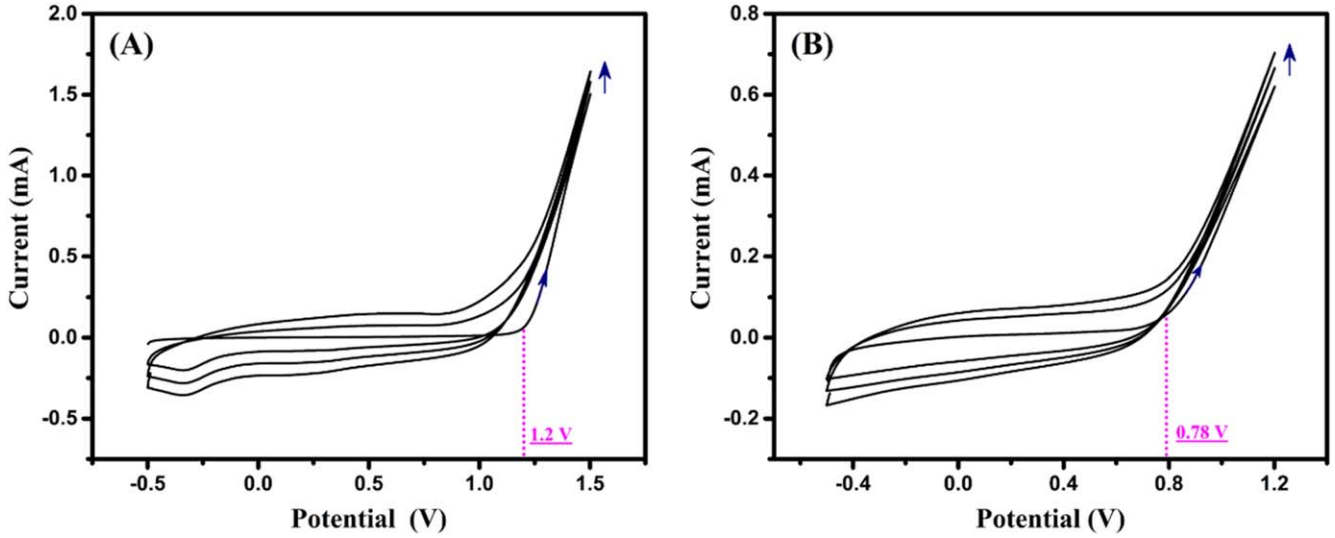


Figure 2. Cyclic voltammograms of EDOT electropolymerization on GCE in (A) ACN + 0.1 M $TBAPF_6$ + 0.05 M EDOT and (B) H_2O + 0.07 M SDS + 0.05 M EDOT. Scan rate: 100 mV s^{-1}.

increases (maximums of 0.16 mA and 0.08 mA for organic and aqueous micellar solution respectively) leading to an electroactive, homogeneous and adherent deposit.

The electrochemical detection of TMZ was then carried out using the two prepared PEDOT films. Initially, PEDOT/ACN and PEDOT/SDS systems were prepared with cyclic voltammetry by varying the number of cycles (3, 5, 8 and 10 cycles), followed by using SWV to characterize the drug. Figure 3 presents the voltammograms obtained for TMZ electrooxidation by GCE without and with modification. As shown, better response was obtained for both systems by applying three voltammetric cycles while a decrease in peak currents was observed when increasing the number of cycles. As already demonstrated for several conducting polymers prepared on oxidizable metals,[36–39] the thickness of the deposit is much higher when increasing the number of applied cycles, hence, the most suitable conclusion to our obtained data is that thin films are the best choice for the electrochemical detection of TMZ. In another way, by increasing the number of cycles, a slow electron transfer rate occurred as a result of surface blockage due to the thick films formed on the electrode surface leading to a low sensitivity of the sensor. In addition, the maximum peak current obtained with three cycles can be attributed to the maximum in effective surface area of the electrode and the electrocatalytic behavior of PEDOT films.[40]

We should note that the electropolymerization of EDOT monomers using one or even two voltammetric cycles has not shown a homogeneous deposit on the electrode surface which could make the electroanalytical characterization of TMZ in this case meaningless.

Moreover, the film prepared in organic medium (Fig. 3A) has bigger sensing properties with much higher peaks compared to the film obtained in micellar solution (Fig. 3B), for this purpose, we focused our study on using PEDOT/ACN for the analytical analysis of TMZ.

The electrochemical response of TMZ using bare GCE and PEDOT/ACN coated GCE was also studied by CV at pH 3.0 in the potential range of −0.25–1.8 V. As presented in Fig. 4, in the absence of TMZ, no peaks were seen with both, bare GCE and GCE/PEDOT/ACN systems. When adding 1×10^{-4} M TMZ to the electrochemical cell, two anodic peaks appeared at 1.1 V (peak 1) and 1.27 V (peak 2) for both systems, however, peaks are well defined only with the system containing the polymer. In addition, a wave was observed at 1.4 V and was not considered for future analyses due to the low sensibility and the hard characterization of this wave. No cathodic peaks were obtained in the reverse scan

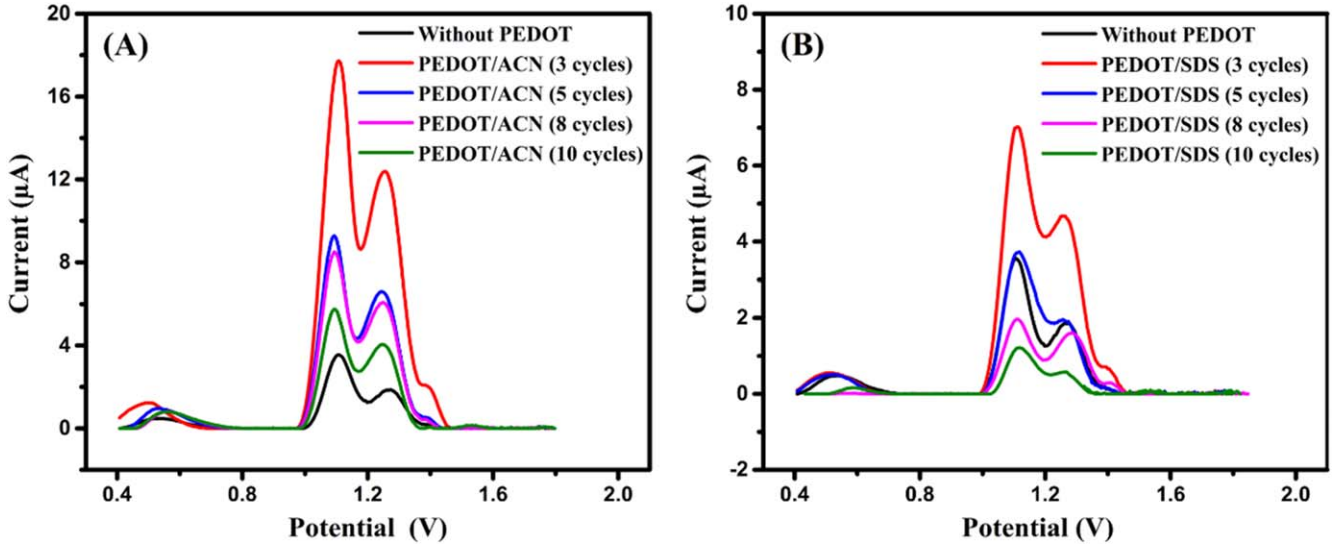


Figure 3. Square wave voltammograms of GCE without and with PEDOT electrosynthesized in (A) ACN and (B) SDS media obtained from 1×10^{-4} M TMZ in phosphate buffer solution (pH 3.0).

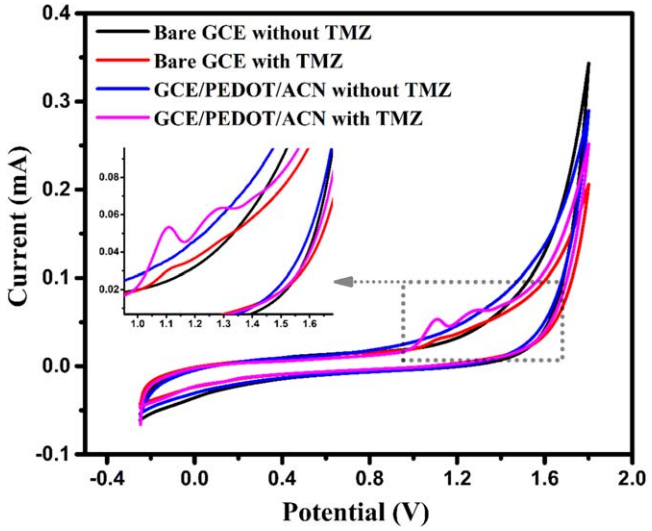


Figure 4. Cyclic voltammograms of different systems with and without 1×10^{-4} M TMZ obtained in phosphate buffer solution (pH 3.0). Scan rate: 100 mV s^{-1}.

suggesting that the oxidation process of TMZ under these experimental conditions is an irreversible one.

Characterization of the PEDOT coating.— *Scanning electron microscopy.*—PEDOT film electrochemically synthesized by cyclic potential scanning between −0.5 and 1.5 V vs Ag/AgCl in {ACN + 0.1 M $TBAPF_6$ + 0.05 M EDOT} on the glassy carbon electrode has been imaged and presented beside bare GCE in Fig. 5.

After a careful mechanical polishing of the GCE surface according to the procedure described previously, we clearly notice the uniform and the smooth surface of the unmodified electrode (Fig. 5, A1, A2). The micrograph observed after the electrodeposition of the polymer shows a homogeneous distribution of the PEDOT coating (Fig. 5, B1), this latter present generally a globular cauliflower structure constituted by microspherical grains of about 1 to 2 μm in diameter (Fig. 5, B2). This common structure-type is one of the important characteristics of conducting polymers, and it was already described in several papers.[41–43]

Infrared spectroscopy.—Oxidized PEDOT film obtained in the organic medium has been analyzed by infrared spectroscopy. The spectrum presented in Fig. 6 is of a good quality and infrared bands are well defined.

The vibrations bands between 1728 and 1375 cm^{-1} are attributed to C=C and C–C stretching modes which originated from the quinoidal structure of PEDOT.[44,45] The absorption bands situated at 670, 816 and 1006 cm^{-1} are due to the vibration of the C–S bonds in the thiophene ring.[46] The peaks appeared at 1044, 1165 and 1289 cm^{-1} are associated to C–O–C bending vibrations in ethylenedioxy group[47] while the band of relatively weak intensity around 962 cm^{-1} is assigned to the ethylenedioxy ring deformation.

On the other hand, the bands located at 536 and 590 cm^{-1} are usually the result of the vibration modes of the doping anion (PF_6^-).[48–50] The presence of these bands confirms the oxidized state of the obtained PEDOT film.

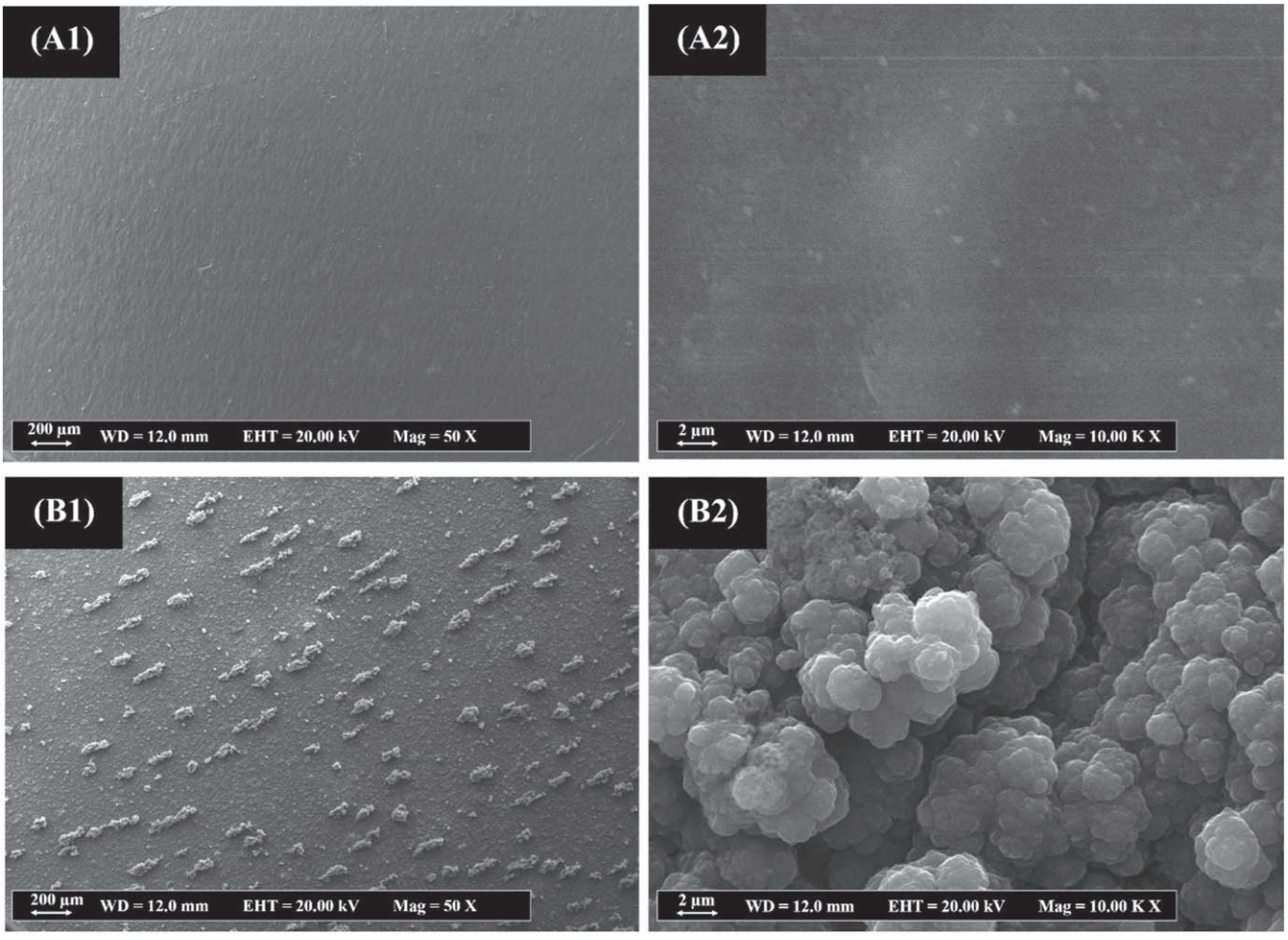


Figure 5. SEM images of (A1, A2) bare GCE and (B1, B2) GCE/PEDOT/ACN.

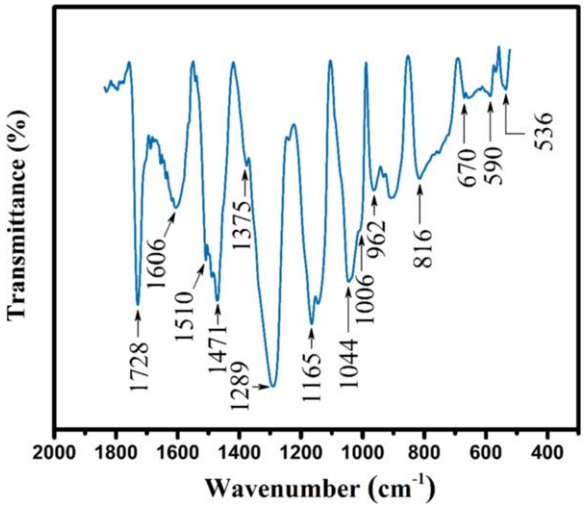


Figure 6. IR spectrum of PEDOT film obtained in {ACN + 0.1 M $TBAPF_6$ + 0.05 M EDOT} medium.

Influence of pH on anodic response of TMZ.—The investigation of pH effect on the anodic response of 1×10^{-4} M TMZ using GCE/PEDOT/ACN was performed by both SWV and DPV. The pH was varied between 1.4 and 7.7 and the corresponding voltammograms are presented in Fig. 7. As we can see, from the two analytical methods used, there is a complex behavior of TMZ electrooxidation when changing the pH. An increase of this latter gives a worthy variation in both, peak current and potential, indicating the pH dependency of TMZ electrooxidation.

No significant shift in potential was observed when using a pH $\leqslant$ 5.1. Knowing that the oxidation mechanism of TMZ is still hard to explain, it's clear to notice the non-similar behavior of TMZ oxidation in acidic media (pH $\leqslant$ 5.1) compared to the one in basic solutions (pH up to 7.7). This was due to the kinds of cations/anions, nature, composition, and concentration of the supporting electrolyte used. Numerous papers have demonstrated that acidic media are the most suitable for the electrochemical characterization of drugs.[40,51,52] In the same context, the electrooxidation of mirtazapine (contain, just as TMZ, a piperazine moiety in its structure), discussed by Ağin et al.,[53] showed one sharp oxidation peak and one additional wave in acidic media in the anodic direction at 1.15 V and 1.3 V respectively; at pH 5.5, mirtazapine gives only a single and sharp peak at about 0.9 V which indicates that the transition from acidic to basic media can provide a total change in the electrooxidation behavior of the drug.

Additionally, well-defined peaks with highest current values are observed in acidic media, especially with phosphate buffer at pH 3.0, thus confirming the conclusion obtained in the preliminary study (section 3.1). A further point is based on the comparison between the voltammograms obtained by the two analytical methods (SWV and DPV), Fig. 7 clearly shows that the SWV technique provides better sensitivity and higher current values, the current response observed with SWV were about 3–4 times higher than those obtained by DPV method,[54] hence, giving a better electroanalytical analysis of TMZ.

Based on the results presented in this section, the electrochemical characterization of TMZ in what follows would be more efficient in phosphate buffer at pH 3.0 using SW voltammetry.

Influence of the cyclic voltammetry scan rate.—In order to understand the nature of interaction between the prepared sensor and TMZ, meaning, to describe whether the oxidation process was diffusion or adsorption controlled, the influence of the scan rate on the electrooxidation of TMZ using GCE/PEDOT/ACN in phosphate buffer at pH 3.0 was carried out by cyclic voltammetry in the range between 5 and 500 mV s^{-1}.

The voltammograms obtained at different scan rates are presented in supplementary Fig. S2. A first look reveals a shift of anodic peak potentials toward more positive values when increasing the scan rate from 5 to 500 mV s^{-1} suggesting the chemical irreversibility of the process[40,55] and therefore confirm the results discussed beforehand.

On the other hand, information about the type of the electron transfer process could be discussed based on the variation of the logarithm of the peak current as a function of the logarithm of the scan rate. Generally, according to several reported works,[56–58] when the plot of log i_p and log ν has a slop of about 0.5, the process is controlled by diffusion while a value of near 1 suggest an adsorption controlled one. As presented in supplementary Fig. S3A, slops of 0.4 and 0.46 for peak 1 and peak 2 respectively were obtained from the two corresponding regression equations suggesting a diffusion-controlled process at the surface of GCE/PEDOT/ACN.[58,59]

The obtained result was supported using the regression data from i_p vs $\nu^{1/2}$ (supplementary Fig. S3B) and i_p vs ν (supplementary Fig. S3C) plots. The linearity of $i_p - \nu^{1/2}$ plots with a correlation coefficient of r = 0.998 and r = 0.997 for peak 1 and peak 2 respectively, and a lower r = 0.960 and r = 0.976 for the same peaks of i_p vs ν equations confirm the diffusion-controlled nature of TMZ electrooxidation process.[58]

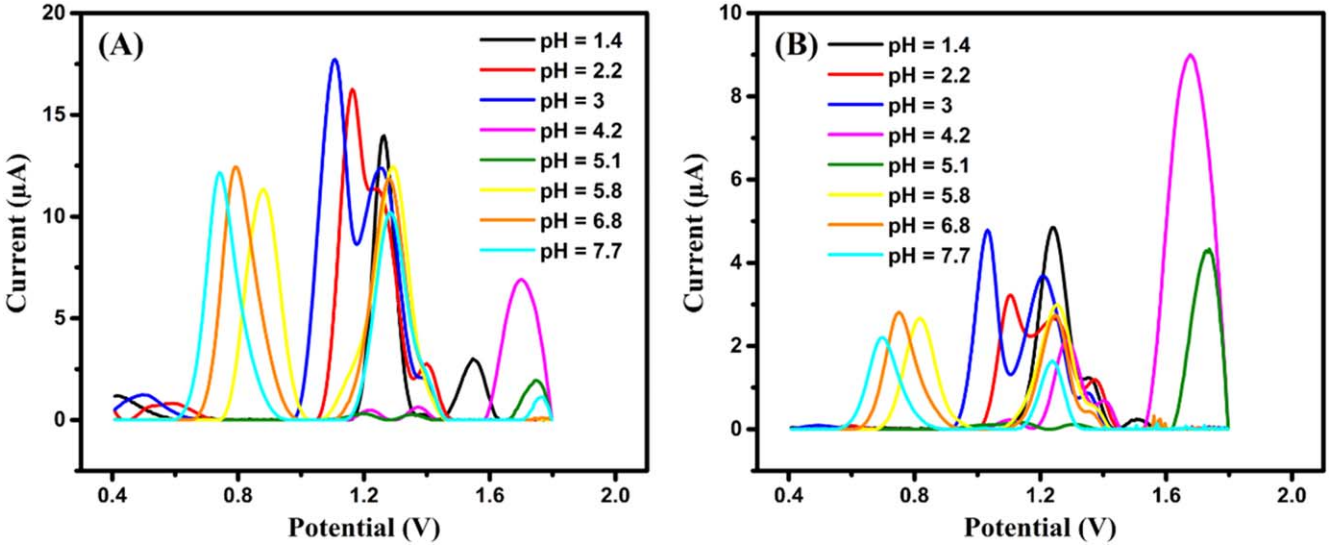


Figure 7. (A) SWV and (B) DPV responses of GCE/PEDOT/ACN obtained from 1×10^{-4} M TMZ in solutions of different pH values.

Optimization of square wave parameters.—We have demonstrated that SWV has the advantage of giving better response compared to DPV technique, hence, to obtain more sensitive voltammograms, the optimum SWV experimental parameters such as frequency (f), pulse amplitude (ΔE_a) and step potential (ΔE_i) were studied.

Electrochemical measurements were achieved using GCE/PEDOT/ACN in phosphate buffer at pH 3.0 containing 1×10^{-4} M TMZ. Each parameter was changed while others were kept constant and the optimum parameters were chosen based on best-shaped and most sensitive signals.

Firstly, by fixing the pulse amplitude at 20 mV and the step potential at 5 mV, the frequency was varied between 10 and 100 Hz. As shown in supplementary Fig. S4A, when increasing the frequency, an instant decrease in peak 1 current was observed while peak 2 gives a slight increase and then a decrease in the current, therefore, the initial frequency value of 10 Hz was found to be the optimum one and was chosen for subsequent experiments.

Pulse amplitude effect was investigated in the range between 10 and 45 mV with constant values of f (10 Hz) and ΔE_i (5 mV). The result presented in supplementary Fig. S4B reveals that, for both peaks, the voltammetric response increases with raising the pulse amplitude up to 25 mV and then the peak current decreases, thus, 25 mV was set as the pulse amplitude.

For step potential, experiments were performed between 3 and 10 mV with 10 Hz frequency and 25 mV pulse amplitude. As seen in supplementary Fig. S4C, an increase in peak currents was obtained when increasing ΔE_i. The maximum response was found at 10 mV, making it the selected one.

As a result of these optimization tests, the SW voltammetric signal was noticeably affected by the experimental parameters. The highest response was recorded at 10 Hz, 25 mV and 10 mV for frequency, pulse amplitude and step potential respectively.

Analytical characterization.— *Calibration curves and reproducibility of the prepared sensor.*—Analytical parameters for TMZ electrooxidation in phosphate buffer at pH 3.0 using the modified electrode were obtained using the optimum condition of SWV method described in the previous part. SW voltammograms for the detection of TMZ at various concentrations are presented in Fig. 8A and the corresponding calibration curves (Fig. 8B) gives a linear relationship between the drug concentration and the anodic peak current in the range of 1×10^{-7} M−1×10^{-4} M with a correlation coefficient greater than 0.997 for both peaks.

Two important parameters, namely, the limit of detection (LOD) and the limit of quantification (LOQ) were also calculated using the two following equations:

$$\mathrm{LOD} = 3\ \mathrm{SD/m};\quad \mathrm{LOQ} = 10\ \mathrm{SD/m}$$

Where SD is the standard deviation calculated from the peak current of the lowest concentration of drug (three times) and m is the slope of the calibration curve.[60,61] LOD and LOQ of 1.20×10^{-8} M and 4.00×10^{-8} M for peak 1 and 1.56×10^{-8} M and 5.22×10^{-8} M for peak 2 respectively were found, meaning the highest sensitivity of the prepared sensor. All analytical characteristics of the corresponding calibration curves are listed in Table I.

In order to investigate the accuracy of the used method, within-day and between-day precisions of GCE/PEDOT/ACN were carried out by measuring, five repetitive time, the peak current and potential in a constant TMZ concentration of 8×10^{-6} M. The calculated relative standard deviations (RSD%) using the following equation were summarized in Table I.

$$\mathrm{RSD}(\%) = (\mathrm{SD/Avg}) \times 100$$

Where SD is the standard deviation and Avg is the average of five measurements (in terms of current or potential values). As noticed, for both, peak currents and potentials, RSD (%) values were less than 2% in within-day and between-day measurements which indicate the high repeatability and reproducibility of the modified electrode.

Interference study.—Selectivity is considered as one of the important characteristics of a sensor to access a practical application, therefore, the effect of some biological compounds like ascorbic acid, dopamine and uric acid present in the extracellular fluid of the central nervous system and some molecules such as NaCl, $CaCl_2$ $MgCl_2$ and $NaNO_3$ usually found in the human body, on the electrooxidation of TMZ was investigated using GCE/PEDOT/ACN. The discussion was based on the change in peak currents using the relative error (RE%) calculated by the equation:

$$\mathrm{RE}(\pm\%) = ((i_{pI} - i_{pB})/ip_B) \times 100$$

Where i_{pI} and i_{pB} are the peak current in the presence and absence of the interferent respectively.[62]

Based on the maximum concentration of foreign species in the electrolytic solution, a relative error of approximately ±5% was

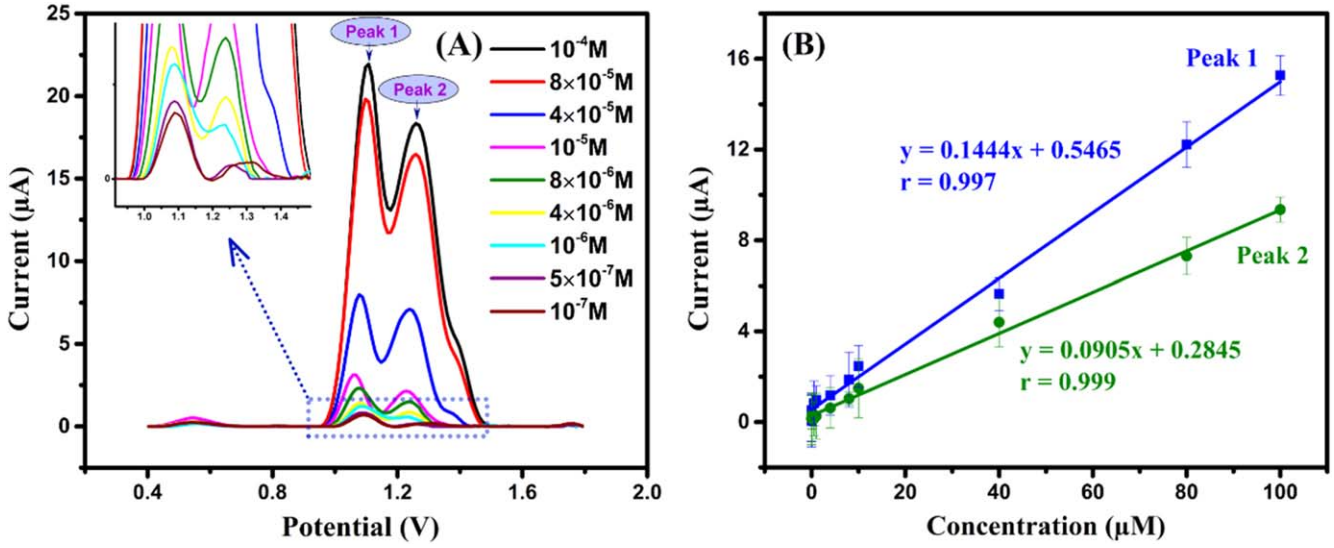


Figure 8. (A) SWV responses of GCE/PEDOT/ACN at various concentrations of TMZ in phosphate buffer solution (pH 3.0) and (B) linear dependency of current vs concentration plots.

Table I. Regression data of calibration lines for quantitative determination of TMZ using GCE/PEDOT/ACN in phosphate buffer solution (pH 3.0).

	Peak 1	Peak 2
Linearity range (M)	1×10^{-7}–1×10^{-4}	
Slope (μA M^{-1})	1.44×10^{5}	9.05×10^{4}
Intercept (μA)	0.5465	0.2845
Correlation coefficient	0.997	0.999
Standard error of slop	3.57×10^{3}	1.26×10^{3}
Standard error of intercept	0.0138	0.0050
LOD (M)	1.20×10^{-8}	1.56×10^{-8}
LOQ (M)	4.00×10^{-8}	5.22×10^{-8}
Within-day of peak current (RSD%)	0.6204	0.30581
Within-day of peak potential (RSD%)	0.9183	0.5606
Between-day of peak current (RSD%)	0.96150	0.7328
Between-day of peak potential (RSD%)	1.2893	0.8153

Table II. Tolerance of interferences on a fixed concentration (4×10^{-5} M) of TMZ using GCE/PEDOT/ACN in phosphate buffer solution (pH 3.0).

		Peak 1		Peak 2	
Foreign substance:TMZ molar ratio		1:1	10:1	1:1	10:1
Relative error (±%)	NaCl	0.29	0.87	0.03	0.88
	$CaCl_2$	0.53	2.28	−0.72	3.12
	$MgCl_2$	1.39	−4.91	−4.40	−5.33
	$NaNO_3$	1.13	−2.86	−2.98	6.48
	Ascorbic acid	1.04	−2.96	0.46	−1.08
	Dopamine	2.89	4.00	2.24	5.36
	Uric acid	−2.07	−6.85	0.44	−1.06

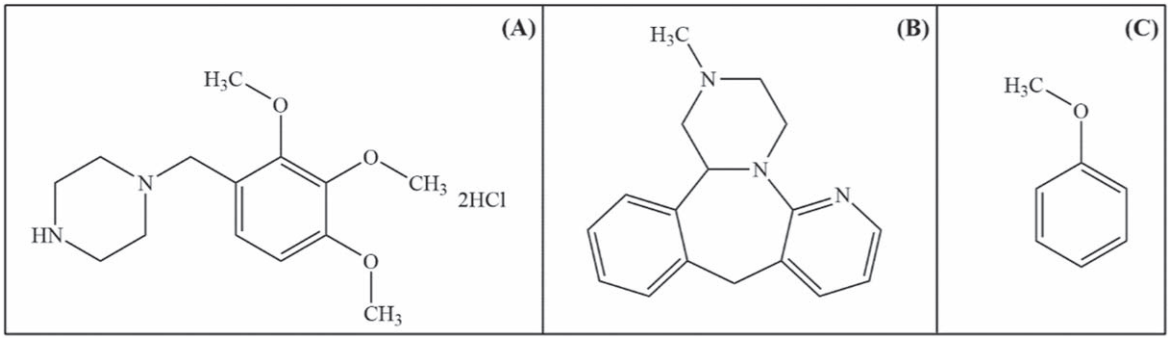
taken as the tolerance limit.[62] Different compounds were introduced separately in molar ratios of 1:1 and 10:1 for foreign substance:TMZ into the electrochemical cell containing 4×10^{-5} M TMZ. From Table II, we can conclude that the presence of these substances in a drug containing-formulation does not cause a significant change in the current (signal change below 5%) except for uric acid and $NaNO_3$ at the molar ratio of 10:1 in which RE values around ±6% were calculated. This may result from their strong adsorption on the surface of the prepared sensor.[63] However, the interference of these two species still not very significant, and the modified electrode has shown a notable selectivity for TMZ detection.

Possible mechanism study.—Although the exact electrooxidation mechanism of TMZ is complex and has not been fully determined, an attempt will be accomplished in order to better understand the oxidation process and to describe the responsible groups for TMZ oxidation. In this context, two different compounds, namely, mirtazapine and anisole, were selected based on their molecular structure which contains groups similar to the ones found in TMZ (Scheme 2).

Cyclic and square wave voltammetric techniques were used for the detection of mirtazapine and anisole in phosphate buffer solution (pH 3.0) using the already prepared polymer (Fig. 9). In addition, for comparative purposes, the result previously found in the case of TMZ was also added to the voltammograms. As shown in Fig. 9, mirtazapine presents a peak at 1.13 V and a wave around 1.30 V, anisole has a peak at 1.50 V while TMZ displays, as mentioned before, two peaks at 1.10 V and 1.27 V and also a wave at about 1.40 V.

The obtained results suggest that the second peak observed in the voltammogram of TMZ is attributed to the oxidation of methoxy groups in anisole molecules.[64] The difference between the two peaks observed in TMZ (1.27 V) and anisole (1.50 V) in terms of shape and potential value may be linked to the piperazine part in TMZ chemical structure which affects the oxidation process. Furthermore, we can also assume that the wave seen at higher potential could be related to the oxidation of that same group.

On the other hand, as already described (section 3.4), mirtazapine showed one sharp oxidation peak and one additional wave in acidic media in the anodic direction at 1.15 V and 1.3 V respectively and were attributed to the oxidation occurred in nitrogen atoms on piperazine and pyridine rings, respectively.[53] In our case, by comparing the first anodic peak of TMZ observed at lower potential (1.10 V) with the one obtained in the voltammogram of mirtazapine



Scheme 2. Molecular structures of (A) trimetazidine, (B) mirtazapine and (C) anisole.

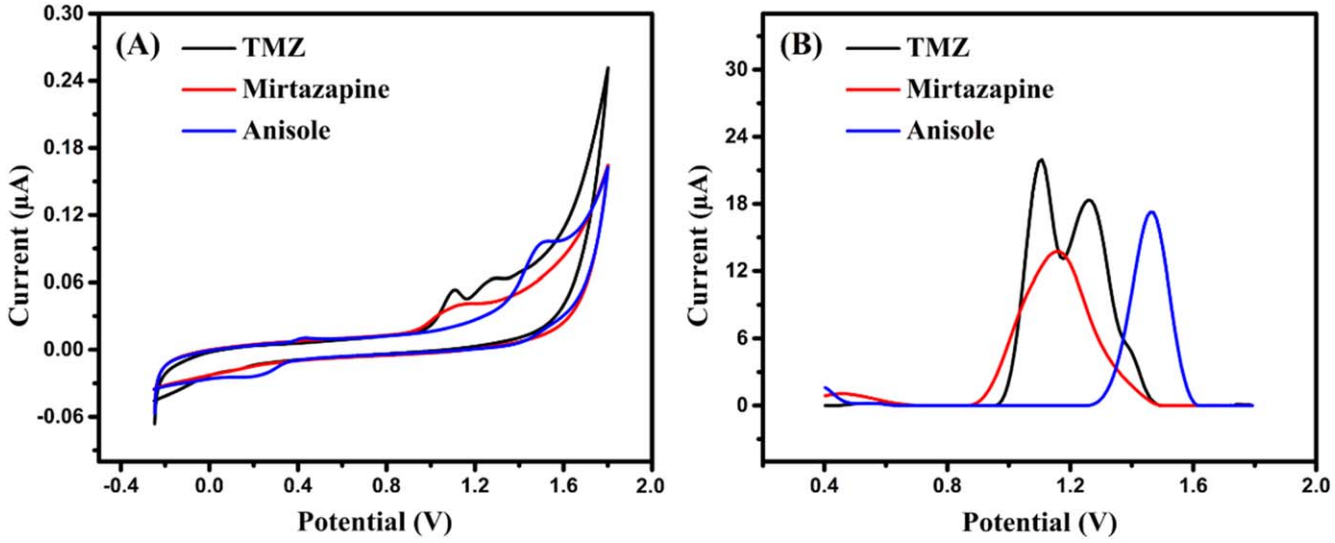


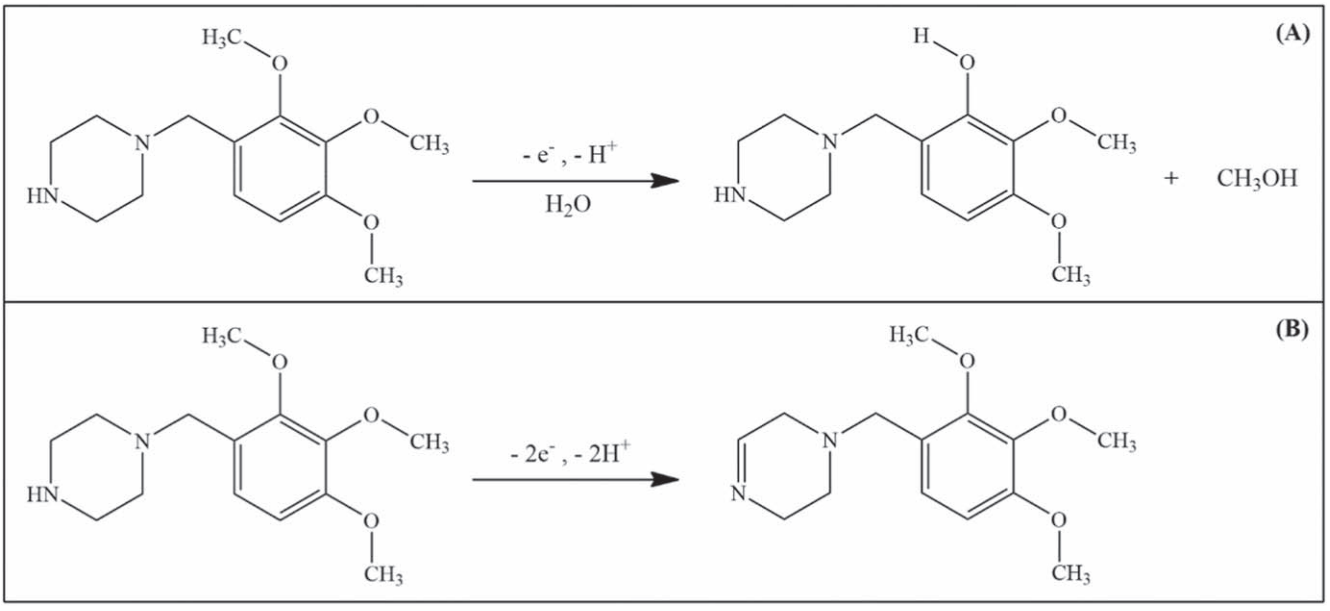
Figure 9. (A) Cyclic and (B) square-wave voltammograms of TMZ, mirtazapine and anisole with a concentration of 1×10^{-4} M using GCE/PEDOT/ACN in phosphate buffer solution (pH 3.0). Scan rate: 100 mV s^{-1}.

(1.13 V) and knowing that the two compounds have piperazine moieties in their structure, it is possible to say that the piperazine part in TMZ molecule is the responsible for the presence of this peak. The oxidation occurs, according to some authors, on nitrogen atoms of piperazine rings by the removal of two protons after the protonation of the secondary amine group.[65] Hence, our study on model compounds indicates that the oxidation mechanism of TMZ using GCE/PEDOT/ACN depends mainly on anisole and piperazine aromatic rings. The proposed reactions are presented in Scheme 3.

Determination of TMZ in biological samples and recovery study.—Taking into account the encouraging results obtained with TMZ electrochemical detection by GCE/PEDOT/ACN in phosphate buffer solution (pH 3.0) as the supporting electrolyte, the analytic measurements were extended to the electrooxidation of TMZ in pharmaceutical formulations aiming to achieve a practical applicability of the proposed method.

SW voltammograms resulted from the determination of TMZ in urine and serum samples are presented in Fig. 10A. As shown, the two main peaks related to TMZ oxidation are present in the three systems (supporting electrolyte, urine and serum). Besides, when using urine, a sharp peak at 0.59 V belongs to uric acid was observed,[66] confirming therefore the used urine containing formulation.

Calibration curves for the detection of pharmaceutical dosage forms of various concentrations of TMZ are also presented in Fig. 10 (B for urine and C for serum). As we can see, a remarkable linearity for both sample and both peaks were obtained with a correlation coefficient $\geqslant$0.996. We should note that, by comparing the analytical parameters gained from calibration curves, peak 1 with the lowest LOD (Table I) is probably the most sensitive one. The same result was found with TMZ detection in serum, the peak 1 gives the biggest linearity range and the lowest LOD compared to the peak 2 (Table III). However, when using urine formulation, it appears that peak 2 is more sensitive in the TMZ oxidation process. It's already mentioned that TMZ electrooxidation in the urine sample illustrates a uric acid peak at lower potential (0.59 V), thus, we can conclude that the presence of this peak could probably affect the peak 1 signal and generates its lowest sensitivity.



Scheme 3. The proposed reactions of TMZ electrooxidation on GCE/PEDOT/ACN related to (A) anisole and (B) piperazine moieties.

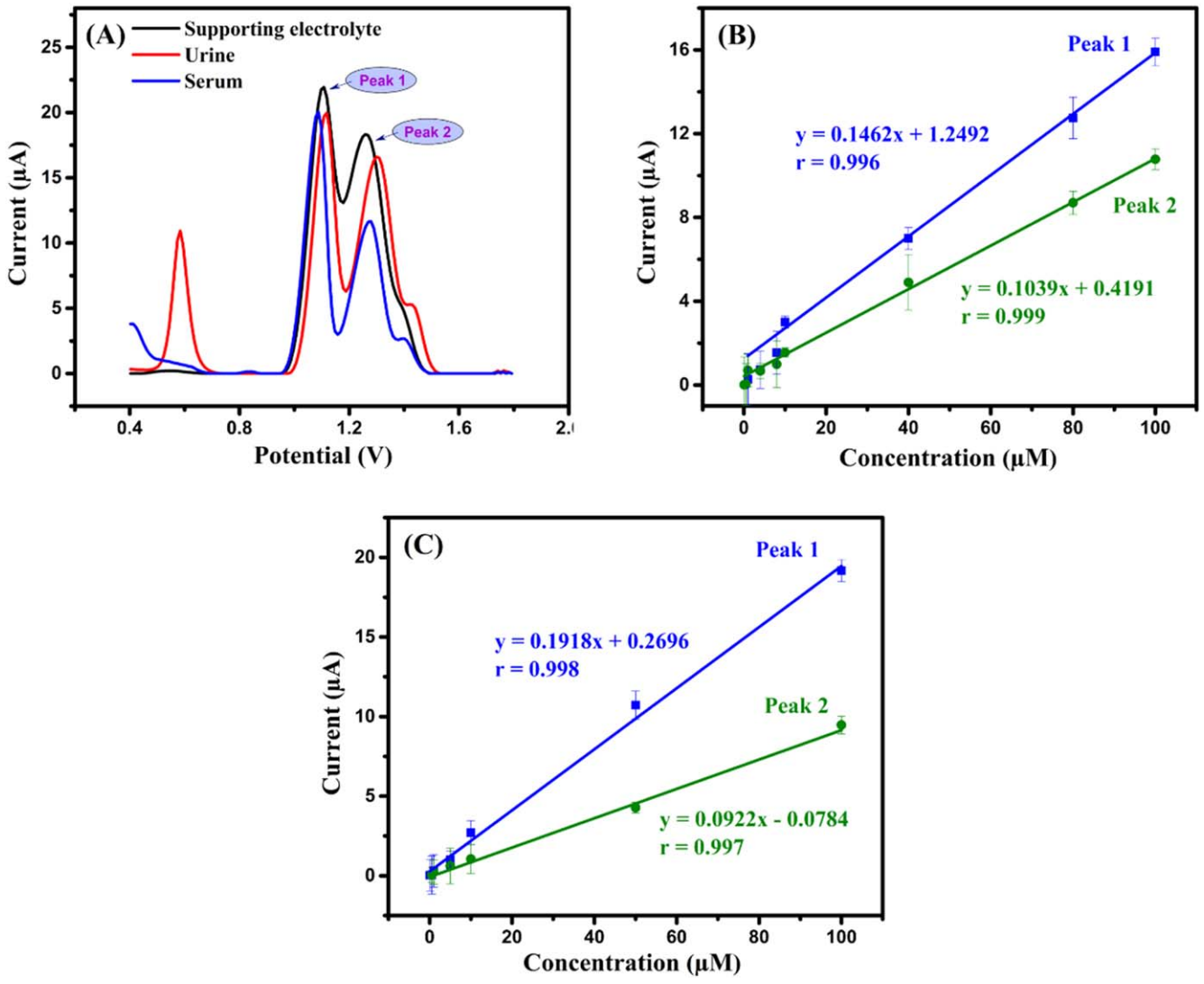


Figure 10. (A) SWV of TMZ (1×10^{-4} M) detection in phosphate buffer solution (pH 3.0), urine and serum samples using GCE/PEDOT/ACN and linear dependency of current vs concentration in (B) urine and (C) serum samples.

Table III. Regression data of calibration lines and recovery analysis for quantitative determination of TMZ in urine and serum samples using GCE/PEDOT/ACN.

	Urine		Serum	
	Peak 1	Peak 2	Peak 1	Peak 2
Linearity range (M)	10^{-6}–10^{-4}	10^{-7}–10^{-4}	10^{-7}–10^{-4}	5×10^{-7}–10^{-4}
Slope (μA M^{-1})	1.46×10^{5}	1.04×10^{5}	1.91×10^{5}	9.22×10^{4}
Intercept (μA)	1.2492	0.4191	0.2696	−0.0783
Correlation coefficient	0.996	0.999	0.998	0.997
Standard error of slop	6.37×10^{3}	1.68×10^{3}	4.91×10^{3}	3.38×10^{3}
Standard error of intercept	0.0261	0.0676	0.0230	0.0175
LOD (M)	5.92×10^{-8}	2.88×10^{-8}	1.80×10^{-8}	6.77×10^{-8}
LOQ (M)	1.97×10^{-7}	9.92×10^{-8}	6.02×10^{-8}	2.25×10^{-7}
Within-day of peak current (RSD%)	0.7252	1.1687	0.4179	0.5652
Within-day of peak potential (RSD%)	0.0393	0.4648	0.0393	0.4694
Between-day of peak current (RSD%)	1.0204	1.8724	1.3018	1.5951
Between-day of peak potential (RSD%)	0.0535	0.5289	0.5428	0.5639
Added (μM)	50	50	60	60
Found (μM)	48.17	47.81	59.58	59.63
Average recovered%	96.34	95.63	99.31	99.39
RSD% of recovery	0.2052	0.5212	0.1393	2.052
Bias%	3.66	4.37	0.69	0.61

Reproducibility and repeatability of TMZ detection in biological samples using GCE/PEDOT/ACN were also investigated and found to be very promising with RSD (%) values less than 2% (Table III). On the other hand, regarding recovery experiments, acceptable percentage values close to 100% were obtained, suggesting the sensitivity and accuracy of the proposed method and the possible applicability of the modified electrode for quantitative analysis of TMZ in real samples.

Conclusions

The modification of the glassy carbon electrode was successfully achieved using an electrodeposition method of PEDOT in aqueous micellar solution (SDS) and organic medium (ACN). The last one offered, after a preliminary study, better detection signals of TMZ. Therefore, the analytical characterization of this drug was realized with GCE/PEDOT/ACN system and the presence of this polymeric coating on the surface of the electrode was confirmed by SEM and IR spectroscopy.

The effect of some important parameters such as pH and scan rate were investigated. The results demonstrated the pH dependency of TMZ oxidation. Moreover, a phosphate buffer solution at pH 3.0 was found, by the SWV method, to be the most suitable medium for TMZ analytical characterization. On the other hand, and based on the linear behavior of log i_p – log ν plots, the electrooxidation process of TMZ was proved to be diffusion controlled.

The influence of interfering compounds was then studied. The analysis gives an acceptable selectivity of the prepared sensor and shows that this method cannot be affected by any foreign species. Regarding the oxidation mechanism of TMZ, model compounds were selected. Consequently, the anisole and piperazine parts of TMZ structures were found to be involved in the oxidation process.

In order to investigate the accuracy of the used method, calibration curves were obtained for the TMZ detection in supporting electrolyte, urine and serum samples. Interesting values of LOD and LOQ and an excellent repeatability and reproducibility of the sensor were established. In addition, when using urine or serum as well-knowns pharmaceutical formulations, recovery values of almost 100% were obtained confirming the good sensitivity, accuracy and selectivity of the modified electrode.

Acknowledgments

This work was supported by the MESRSFC and CNRST (Morocco) under grant no. PPR/30/2015. Thanks to expressed to GM Pharma for supporting this study with obtaining drug.

ORCID

Abdelqader El Guerraf https://orcid.org/0000-0002-5221-8656
Nurgul K. Bakirhan https://orcid.org/0000-0001-5469-9142

References

1. A. Onay-Besikci and S. A. Özkan, *Cardiovasc. Ther.*, **26**, 147 (2008).
2. A. Medvedovici, F. Albu, C. Georgiţă, and V. David, *Biomed. Chromatogr.*, **19**, 549 (2005).
3. C. Harpey, P. Clauser, C. Labrid, J.-L. Freyria, and J.-P. Poirier, *Cardiovasc. Drug Rev.*, **6**, 292 (1988).
4. J. Ancerewicz et al., *Free Radic. Biol. Med.*, **25**, 113 (1998).
5. M. Ghoneim, P. Khashaba, and A. Beltagi, *J. Pharm. Biomed. Anal.*, **27**, 235 (2002).
6. E. G. C. Clarke, *J. Med. Chem.*, **13**, 338 (1970).
7. L. P. Palilis and A. C. Calokerinos, *Anal. Chim. Acta*, **413**, 175 (2000).
8. L. Fay, G. Michel, P. Goupit, C. Harpey, and M. Prost, *J. Chromatogr. B Biomed. Sci. Appl.*, **490**, 198 (1989).
9. P. J. Jackson, R. D. Brownsill, A. R. Taylor, G. Resplandy, B. Walther, and H. R. Schwietert, *Xenobiotica*, **26**, 221 (1996).
10. S. Courte and N. Bromet, *J. Chromatogr. B Biomed. Sci. Appl.*, **224**, 162 (1981).
11. V. R. Bari, U. J. Dhorda, and M. Sunderesan, "Trace determination of trimetazidine hydrochloride in human blood plasma by HPLC using electrochemical detection", *Indian Drugs*, **36**, 289 (1999).
12. S. O. Thoppil and P. Amin, *J. Pharm. Biomed. Anal.*, **25**, 191 (2001).
13. A. El Jaouhari et al., *Synth. Met.*, **226**, 15 (2017).
14. M. J. García-Fernández, S. Sancho-Querol, M. M. Pastor-Blas, and A. Sepúlveda-Escribano, *J. Colloid Interface Sci.*, **494**, 98 (2017).
15. Z. L. Long, Y. C. Zhou, and L. Xiao, *Appl. Surf. Sci.*, **218**, 124 (2003).
16. K. Gurunathan, D. P. Amalnerkar, and D. C. Trivedi, *Mater. Lett.*, **57**, 1642 (2003).
17. A. El Guerraf, Z. Aouzal, M. Bouabdallaoui, S. Ben Jadi, A. El Jaouhari, R. Wang, M. Bazzaoui, and E. A. Bazzaoui, *J. Solid State Electrochem.*, **23**, 1811 (2019).
18. H. Randriamahazaka, V. Noël, and C. Chevrot, *J. Electroanal. Chem.*, **521**, 107 (2002).
19. M. del Valle, P. Cury, and R. Schrebler, *Electrochim. Acta*, **48**, 397 (2002).
20. S. Sadki and C. Chevrot, *Electrochim. Acta*, **48**, 733 (2003).
21. Y. Seekaew, S. Lokavee, D. Phokharatkul, and A. Wisitsoraat, *Org. Electron.*, **15**, 2971 (2014).
22. T. Galán, B. Prieto-Simón, M. Alvira, R. Eritja, G. Götz, P. Bäuerle, and J. Samitier, *Biosens. Bioelectron.*, **74**, 751 (2015).
23. H. Randriamahazaka, V. Noël, and C. Chevrot, *J. Electroanal. Chem.*, **472**, 103 (1999).
24. B. Rasch and W. Vielstich, *J. Electroanal. Chem.*, **370**, 109 (1994).
25. V. Noël, H. Randriamahazaka, and C. Chevrot, *J. Electroanal. Chem.*, **542**, 33 (2003).
26. C. Kvarnström, H. Neugebauer, S. Blomquist, H. J. Ahonen, J. Kankare, and A. Ivaska, *Electrochim. Acta*, **44**, 2739 (1999).
27. M. Dietrich, J. Heinze, G. Heywang, and F. Jonas, *J. Electroanal. Chem.*, **369**, 87 (1994).
28. G. A. Sotzing, J. L. Reddinger, J. R. Reynolds, and P. J. Steel, *Synth. Met.*, **84**, 199 (1997).
29. R. Schweiss, J. F. Lübben, D. Johannsmann, and W. Knoll, *Electrochim. Acta*, **50**, 2849 (2005).
30. N. Sakmeche, S. Aeiyach, J. J. Aaron, M. Jouini, J. C. Lacroix, and P. C. Lacaze, *Langmuir*, **15**, 2566 (1999).
31. E. A. Bazzaoui, S. Aeiyach, and P. C. Lacaze, *J. Electroanal. Chem.*, **364**, 63 (1994).
32. A. Lima, P. Schottland, S. Sadki, and C. Chevrot, *Synth. Met.*, **93**, 33 (1998).
33. N. Sakmeche, J.-J. Aaron, S. Aeiyach, and P.-C. Lacaze, *Electrochim. Acta*, **45**, 1921 (2000).
34. C. Stromberg, V. Tsakova, and J. Schultze, *J. Electroanal. Chem.*, **547**, 125 (2003).
35. N. Sakmeche, J. J. Aaron, M. Fall, S. Aeiyach, M. Jouini, J. C. Lacroix, and P. C. Lacaze, *Chem. Commun.*, **2723**, 2723 (1996), (http://xlink.rsc.org/?DOI=cc9960002723).
36. M. Bazzaoui, L. Martins, E. A. Bazzaoui, and J. I. Martins, *Electrochim. Acta*, **47**, 2953 (2002).
37. M. Bazzaoui, J. I. Martins, S. C. Costa, E. A. Bazzaoui, T. C. Reis, and L. Martins, *Electrochim. Acta*, **51**, 2417 (2006).
38. N. C. T. Martins, T. Moura, E. Silva, M. F. Montemor, J. C. S. Fernandes, and M. G. S. Ferreira, *Electrochim. Acta*, **53**, 4754 (2008).
39. M. A. Del Valle, F. R. Díaz, M. E. Bodini, T. Pizarro, R. Córdova, H. Gómez, and R. Schrebler, *J. Appl. Electrochem.*, **28**, 943 (1998).
40. S. Aftab, G. Ozcelikay, S. Kurbanoglu, A. Shah, F. J. Iftikhar, and S. A. Ozkan, *J. Pharm. Biomed. Anal.*, **165**, 73 (2019).
41. S. Patra and N. Munichandraiah, *J. Appl. Polym. Sci.*, **106**, 1160 (2007).
42. G. Tourillon and F. Garnier, *J. Polym. Sci. Polym. Phys. Ed.*, **22**, 33 (1984).
43. A. A. Hermas, S. S. Al-Juaid, S. A. Al-Thabaiti, A. H. Qusti, and M. A. Salam, *Prog. Org. Coatings*, **75**, 404 (2012).
44. S. V. Selvaganesh, J. Mathiyarasu, K. L. N. Phani, and V. J. N. R. L. Yegnaraman, *Nanoscale Res. Lett.*, **2**, 546 (2007).
45. Y. Ma, F. Zhao, and B. Zeng, *Talanta*, **104**, 27 (2013).
46. Q. Xie et al., (2016), (eds.)*PLoS One*, **11**, e0166529.
47. C. Li and T. Imae, *Macromolecules*, **37**, 2411 (2004).
48. A. M. Fenelon and C. B. Breslin, *J. Electrochem. Soc.*, **152**, D6 (2005).
49. D. Gambino, E. Kremer, E. J. Baran, and A. Mombru, *Zeitschrift für Anorg. und Allg. Chemie*, **3**, 813 (1999).
50. A. Milton Franklin Benial, V. Ramakrishnan, and R. Murugesan, *Spectrochim. Acta Part A Mol. Biomol. Spectrosc.*, **58**, 1703 (2002).
51. A. Zahid, N. K. Bakirhan, L. Karadurmuş, A. Shah, and S. A. Ozkan, *Electroanalysis*, **31**, 1598 (2019).
52. B. Uslu and S. A. Özkan, *Electrochim. Acta*, **49**, 4321 (2004).
53. F. Ağin, N. Karada, B. Uslu, and S. A. Özkan, *Maced. J. Chem. Chem. Eng.*, **32**, 41 (2013).
54. V. Mirceski, S. Komorsky-Lovric, and M. Lovric, *Square-Wave Voltammetry* (Springer, Berlin, Heidelberg) (2007), https://www.springer.com/gp/book/9783540737391.
55. B. Dogan-Topal, N. K. Bakirhan, T. T. Tok, and S. A. Ozkan, *Electroanalysis*, **31**, 1 (2019).
56. D. K. Gosser, *Cyclic Voltammetry* (VCH, New York) (1994).
57. E. Laviron and L. Roullier, *J. Electroanal. Chem. Interfacial Electrochem.*, **115**, 65 (1980).
58. N. Karadas, S. Sanli, M. Gumustas, and S. A. Ozkan, *J. Pharm. Biomed. Anal.*, **66**, 116 (2012).
59. E. Laviron, *J. Electroanal. Chem. Interfacial Electrochem.*, **112**, 1 (1980).
60. J. Ermer and J. H. John, "Method validation in pharmaceutical analysis : A guide to best practice." ed. J. Ermer and J. H. M. C. B. Miller (Wiley, New York) p. 1 (2006), (https://onlinelibrary.wiley.com/doi/book/10.1002/3527604685).
61. S. A. Ozkan, *Electroanalytical Methods in Pharmaceutical Analysis and Their Validation* (H N B Pub, New York, United States) (2011).
62. H. Lin, G. Li, and K. Wu, *Food Chem.*, **107**, 531 (2008).
63. N. K. Bakirhan, M. S. B. Celik, H. Celik, B. Uslu, and S. A. Ozkan, *Electroanalysis*, **30**, 2273 (2018).
64. Z. Shi, J. Tan, Y. Hu, G. Li, and X. Xiao, *Electroanalysis*, **30**, 2467 (2018).
65. A. K. Ateş, E. Er, H. Çelikkan, and N. Erk, *Microchem. J.*, **148**, 306 (2019).
66. X. Tian, C. Cheng, H. Yuan, J. Du, D. Xiao, S. Xie, and M. M. F. Choi, *Talanta*, **93**, 79 (2012).